ACS APPLIED POLYMER MATERIALS

pubs.acs.org/acsapm

Article

Uniformly Dispersed Poly(lactic acid)-Grafted Lignin Nanoparticles Enhance Antioxidant Activity and UV-Barrier Properties of Poly(lactic acid) Packaging Films

Alice Boarino, Aigoul Schreier, Yves Leterrier, and Harm-Anton Klok*

Cite This: *ACS Appl. Polym. Mater.* 2022, 4, 4808−4817

Read Online

ACCESS | Metrics & More | Article Recommendations | Supporting Information

ABSTRACT: Poly(lactic acid) (PLA) represents one of the most widely used biodegradable polymers for food packaging applications. While this material provides many advantages, it is characterized by limited antioxidant and UV-barrier properties. Blending PLA with lignin is an attractive strategy to address these limitations. Lignin possesses antioxidant properties and absorbs UV-light and is a widely available low value byproduct of the paper and pulp industry. This study has explored the use of lignin nanoparticles to augment the properties of PLA-based films. A central challenge in the preparation of PLA−lignin nanoparticle blend films is to avoid nanoparticle aggregation, which could compromise optical properties as well as antioxidant activity, among others. To avoid nanoparticle aggregation in the PLA matrix, PLA-grafted lignin nanoparticles were prepared via organocatalyzed lactide ring-opening polymerization. In contrast to lignin and unmodified lignin nanoparticles, these PLA-grafted lignin nanoparticles could be uniformly dispersed in PLA for lignin contents up to 10 wt %. The addition of as little as the equivalent of 1 wt % of lignin of these nanoparticles effectively blocked transmission of 280 nm UV-light. At the same time, these blend films retained reasonable visible light transmittance. The optical properties of the PLA lignin blend films also benefited from the well-dispersed nature of the PLA-grafted nanoparticles, as evidenced by significantly higher visible light transmittance of blends of PLA and PLA-grafted nanoparticles, as compared to blends prepared from PLA with lignin or unmodified lignin nanoparticles. Finally, blending PLA with PLA-grafted lignin nanoparticles greatly augments the antioxidant activity of these films.

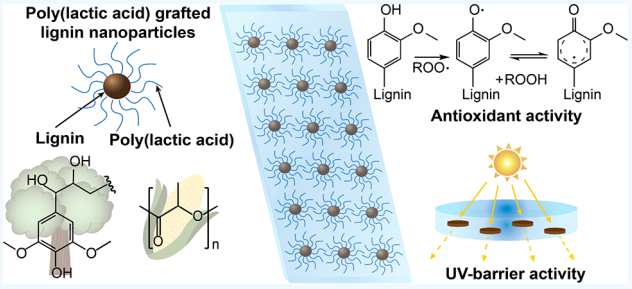

KEYWORDS: *poly(lactic acid), lignin nanoparticles, food packaging, antioxidant, UV-barrier*

INTRODUCTION

Currently, more than 300 million tons of plastic are globally produced every year. Around 50% of these polymers are used as packaging materials.[1,2] The vast majority of these polymers are generated from petroleum-based resources, for example, polyethylene (PE), poly(ethylene terephthalate) (PET), polypropylene (PP), polystyrene (PS), and poly(vinyl chloride) (PVC).[3] Polymers based on renewable resources represent only 1% of this amount.[4] However, together with the growing demand for greener and more sustainable materials, the biopolymers market is in continuous expansion.[4] Polymers such as poly(lactic acid) (PLA) are excellent alternatives to conventional petroleum-based plastics, as they are derived from biorenewable sources and can be enzymatically or hydrolytically degraded.[5] PLA is one of the most widely used degradable polymers for packaging applications.[6] It is accepted as GRAS (Generally Recognized as Safe) by the Food and Drug Administration (FDA) and is particularly suitable for use in food and beverage packaging applications.[7]

Packaging materials serve to protect food from the effects of exposure to oxygen, water vapor, ultraviolet light, and chemical as well as microbiological contamination, which can reduce food shelf life. Oxidation of food can lead to organoleptic changes, such as off-odors, off-flavours, texture, and color changes, as well as to the formation of toxic compounds such as aldehydes, and the loss of nutritional value.[8] To prevent food oxidation, antioxidants such as butylated hydroxyanisole and butylated hydroxytoluene, which act as oxygen radical scavenger, can be incorporated in the packaging material.[9] A drawback of these antioxidants, however, is that they may lead to the generation of carcinogenic compounds, resulting in other adverse side effects on human health, such as allergies caused by benzoic acid, nitrates, and sulfites.[10,11] To overcome these challenges, there is a growing interest in exploring natural

Received: March 11, 2022
Accepted: May 16, 2022
Published: May 24, 2022

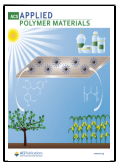

antioxidants from plant leaves, spices, and herbs, which are presumably safer for human consumption. One interesting sustainable and low-cost alternative to non-renewable toxic antioxidants is lignin.[12−14] Every year, 70 million tons of lignin are isolated as byproducts of the paper and pulp industry, and most of it is burned as a low-value fuel.[15,16] In addition to being biocompatible[17−19] and providing antioxidant activity, lignin also absorbs UV-light and thus allows to impart UV-barrier properties on food packaging materials.[19−22]

While PLA offers many advantages, it suffers from limited antioxidant and UV-barrier properties. Blending PLA with lignin would provide a possibility to improve the antioxidant[14,23,24] and UV-barrier properties of the polymer.[25−27] PLA lignin blends, however, phase separate.[25,28−31] In addition to blending lignin, another approach to enhance the properties of PLA involves the incorporation of lignin nanoparticles. PLA−lignin nanoparticle blend films are attractive due to the small size and high surface-area-to-volume-ratio of the nanoparticles, which is interesting with respect to optical and antioxidant properties.[32−37] Lignin nanoparticles incorporated in PLA, however, also aggregate, which reduces the potential beneficial effects of their high surface-area-to-volume ratio on enhancing the properties of PLA and which may also impact the diffusion barrier properties of the composite.

To enhance the dispersion of lignin nanoparticles in PLA, this study explores the use of PLA-grafted lignin nanoparticles. This report outlines the synthesis of PLA-modified lignin nanoparticles and compares the morphology of blends of PLA and PLA-grafted lignin nanoparticles with those of blends prepared by mixing PLA and unmodified lignin nanoparticles or lignin as well as pure PLA films. Subsequently, the mechanical, oxygen, and water vapor barrier properties, as well as the optical properties and antioxidant activities of blends of PLA and PLA-grafted nanoparticles, are compared with those of blends prepared from PLA with lignin or unmodified lignin nanoparticles.

EXPERIMENTAL SECTION

Materials. All chemicals were used as received unless described otherwise. Soda lignin (Protobind 1000) was purchased from Tanovis AG, Switzerland. Food packaging grade poly(lactic acid) (Ingeo biopolymer 4060D) was purchased from NatureWorks LLC, USA. This PLA has a weight-average molecular weight (M_w) of 190000 g/mol and contains 12 mol % D-lactide, as provided by the supplier. All other reagents were purchased from Sigma-Aldrich. Dichloromethane (DCM) and chloroform ($CHCl_3$) were purified and dried by using a solvent-purification system (PureSolv). Deionized water was obtained from a Millipore Direct-Q 5 ultrapure water system.

Methods. *Nuclear Magnetic Resonance (NMR) Spectroscopy.* NMR spectra were recorded on a Bruker AVANCE III 400 MHz spectrometer. For ^{1}H NMR and diffusion-ordered spectroscopy (DOSY)-NMR, samples were dissolved in deuterated dimethylformamide (DMF) at a concentration of 10 mg/mL. Chemical shifts are reported relative to the residual solvent signal. For ^{31}P NMR, lignin hydroxyl groups were reacted with 2-chloro-4,4,5,5-tetramethyl-1,3,2-dioxaphospholane (TMDP) as a phosphorylation agent. Around 20 mg of sample was precisely weighted and stirred overnight at room temperature in 400 μL of a 0.8:0.8:1 v/v mixture of deuterated CH_3Cl, deuterated DMF, and anhydrous pyridine, containing 4 mg of chromium(III) acetylacetonate as a relaxation agent and 0.082 mmol of cyclohexanol as an internal standard. Then, 100 μL of TMDP was added, and the mixture was stirred for 8 h at room temperature. Because TMDP is moisture-sensitive, the reaction was performed under an argon atmosphere to avoid exposure to air and water. The solution was finally transferred into an NMR tube, sealed with a septum, and previously purged with argon.

Atomic Force Microscopy (AFM). Samples for AFM were prepared on silicon wafers (10 mm × 8 mm size) cleaned via sonication in methanol, deionized water, and acetone for 10 min each. The substrates were then placed in a Femto Oxygen Plasma system (200 W, Diener Electronic) under 5 mL/min oxygen flow for 15 min. AFM images were recorded using an Asylum Research Cypher VRS instrument (Oxford Instruments, United Kingdom). Measurements were done in tapping mode using a trihedral aluminum-coated silicon cantilever (HQ:NSC14/Al BS, MikroMasch, Hungary) with a spring constant of 5 N/m and a resonance frequency of ∼160 kHz. To determine nanoparticle sizes and size distributions, 4 μL of a nanoparticle dispersion in $CHCl_3$ (concentration 0.1 mg/mL) was deposited on a silicon wafer. The wafers were dried overnight at room temperature and then imaged. Images were processed with the Gwyddion software. The reported particle sizes are the average of 50 nanoparticle heights. To study the morphology of polymer blend films, 10 μL of polymer solution in $CHCl_3$ (polymer concentration 10 wt %) was spin-coated on the surface of a silicon wafer by a Convac ST 146 spin-coater (2000 rpm, 100 s) and then dried overnight at room temperature.

Scanning Electron Microscopy (SEM). SEM imaging was performed on a ZEISS Gemini SEM 3000 scanning electron microscope. Before image acquisition, the films were first embedded in resin (Epoxy Embedding Medium EPON 812, Sigma-Aldrich) and then cured overnight in an oven at 60 °C. After that, 1 μm thick specimens were cut by using ultramicrotomy and were coated with a 10 nm thick layer of carbon to reduce charging effects.

UV−Vis Spectroscopy. To quantify the lignin content (wt %) of the PLA-grafted nanoparticles, first a calibration curve was established by recording the UV−vis absorbance at 280 nm of solutions of lignin nanoparticles dissolved in DMF (concentration 0−50 μg/mL) by using a PerkinElmer Lambda 365 UV−vis spectrophotometer (Supporting Information Figure S1). Lignin contents of solutions of PLA-grafted lignin nanoparticles of known concentration were determined by using this calibration curve by measuring the UV absorbance at 280 nm. To measure the UV-barrier properties and transparency of polymer films in the visible range, light transmittance spectra in the wavelength of 200−700 nm were recorded.

Thermal Analysis. Thermogravimetric analysis (TGA) was performed using a PerkinElmer TGA 400 instrument. Experiments were conducted under a nitrogen atmosphere by increasing the temperature from 30 to 800 °C at a heating rate of 1 °C/min. Differential scanning calorimetry (DSC) measurements were executed using a DSC 8000 instrument from PerkinElmer, which was calibrated with water, indium, and zinc as standards. Each sample was first heated from 20 to 220 °C at a rate of 10 °C/min to erase any previous thermal history and then rapidly cooled to 20 °C in 6 min, prior to a second heating scan (from 20 to 220 °C at a rate of 10 °C/min).

Oxygen and Water Vapor Permeability Measurement. Oxygen transmission rates (OTR) were determined at 23 °C and 50% relative humidity by using a coulometric cell (Systech 8001, United Kingdom), with a measurement limit of 0.008 cm^3/m^2/day. For each sample, two films were mounted in the two chambers of the apparatus with a circular opening of 5 cm^2. After purging the chambers with nitrogen until baseline stabilization, one side of the films was exposed to an oxygen gas flow (1 bar), and the OTR value was obtained by the mean of the data collected from the two chambers. The water vapor transmission rate (WVTR) was measured by using the same method and conditions reported for the OTR by using an electrolytic P_2O_5 sensor (Systech 7001, United Kingdom), with a measurement limit of 0.02 g/m^2/day. A water vapor flow was applied to one side of the films during the experiment.[38] The permeability to oxygen (OP) and water vapor (WVP) was calculated from the respective transmission rate as

https://doi.org/10.1021/acsapm.2c00420
ACS Appl. Polym. Mater. 2022, 4, 4808−4817

Scheme 1. Synthesis of Lignin Nanoparticles and Subsequent Grafting of Poly(lactic acid) (PLA) via Lactide Ring-Opening Polymerization

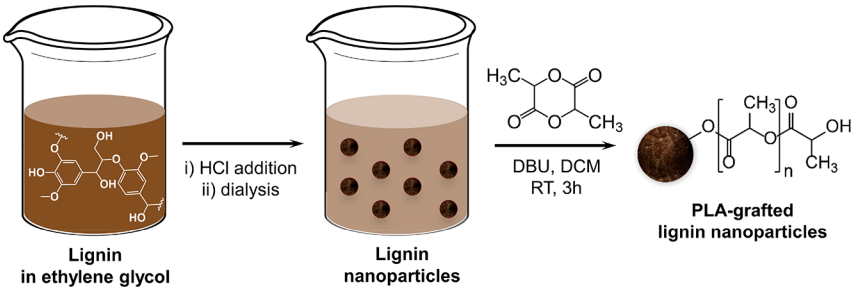

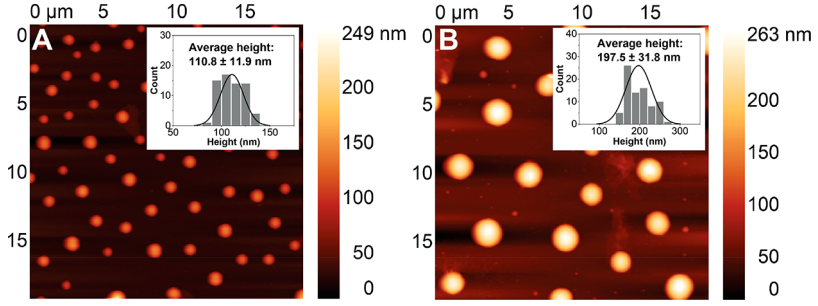

Figure 1. AFM images and size distributions of (A) lignin nanoparticles and (B) PLA-modified lignin nanoparticles that were prepared with an initial lactide/lignin nanoparticle ratio of 5/1 (w/w).

$$\text{OP} = \text{OTR} \times h \text{ and WVP} = \text{WVTR} \times \frac{h}{\text{saturated pressure} \times \%\text{RH}}$$

where h is the thickness of the film, the water saturation pressure at 23 °C is 3.17 kPa, and the relative humidity is 50%.[39] For the film thickness, the average of five values obtained with a micrometer was considered.

Mechanical Testing. The tensile properties of the films were measured using an Instron 1011 universal testing machine, equipped with a 5 kN load cell in accordance with ASTM D638. The specimens had a length, width, and thickness of narrow section of 165, 10, and 1 mm, respectively. These dimensions are in accordance with specimen Type I as reported in the ASTM D638. Five specimens were tested for each blend at a constant speed of 5 mm/min.

Statistical Analyses. The data are presented as mean ± standard deviation of the mean. The Student's t test statistical difference was performed, and differences between the data are considered statistically significant at $^{*}p < 0.05$, $^{**}p < 0.01$, and $^{***}p < 0.001$.

Procedures. *Lignin Nanoparticle Synthesis.* Lignin nanoparticles were prepared via precipitation.[40] First, a solution of 4 wt % lignin in ethylene glycol was prepared by dissolving 0.888 g of lignin in 20 mL of ethylene glycol. The solution was stirred for 2 h at room temperature and then filtered through a filter paper (Whatman 541, pore size 22 μm) to remove the insoluble lignin impurities. Then, using a peristaltic pump, 1 mL of 0.25 M HCl was added to the lignin solution at a rate of 0.04 mL/min under vigorous stirring. After the addition of the acid was completed, stirring was continued for another 2 h, followed by sonication for 30 min at a frequency of 30 kHz in a TPC-40 ultrasonic bath (Telsonic AG, Switzerland), and then dialysis against 2 L water through a membrane with cutoff of 10 kDa. Dialysis was performed for 3 days changing the water three times daily, resulting in a final solution pH of 7 as measured with a pH meter (Seven Easy, Mettler Toledo, USA). Finally, the water was removed by freeze-drying for a period of 48 h to obtain nanoparticles in 30% yield.

Synthesis of PLA-Grafted Lignin Nanoparticles. In a typical experiment, 300 mg of lignin nanoparticles, 1.5 g of DL-lactide (11.5 mmol), and 50 mg of 1,8-diazabicyclo[5.4.0]undec-7-ene (DBU) (0.33 mmol) were added to a 50 mL Schlenk flask. Then, 20 mL of anhydrous DCM was added, and the reaction mixture was stirred under N_2 at room temperature for 3 h. After that, the reaction was quenched with 0.5 mL of acetic acid, and the crude product precipitated by addition of 160 mL of methanol. The final product was isolated by centrifugation (20 min, 8000 rpm, three times) and then dried in a vacuum oven at 60 °C overnight.

Preparation of PLA Blend Films. Films of blends of PLA with lignin, lignin nanoparticles, and PLA-modified lignin nanoparticles were prepared via solvent casting. Films were prepared that contained 1, 5, and 10 wt % lignin. First, PLA was dried overnight at 40 °C in a vacuum oven. Then, it was dissolved in chloroform at a concentration of 10 wt % with vigorous stirring at room temperature for 12 h. At the same time, the lignin, lignin nanoparticles, or PLA-grafted lignin nanoparticles were stirred in chloroform (concentration 10 mg/mL) for 12 h as well. The PLA solutions and lignin dispersions were then mixed and stirred overnight. The mixture was finally cast onto a Teflon Petri dish. The lignin content of the blend films was varied by adjusting the volumes of the PLA solution and the lignin dispersions. The film was left drying for 24 h at room temperature, under the fume hood, and finally for 72 h in a vacuum oven at 50 °C.

DPPH Assay. The antioxidant activity of the samples was evaluated using the 2,2-diphenyl-1-picrylhydrazyl (DPPH) colorimetric assay, with a slightly modified version of the method reported by Blois.[41] For these experiments, 40 mg of each film was cut into small pieces and immersed in 2 mL of a 25 mg/L DPPH solution in methanol. The samples were shaken in the dark for 3 h, and their absorbance at 517 nm was measured. The DPPH radical-scavenging activity is calculated as

$$\text{antioxidant activity (\%)} = \frac{A_0 - A_t}{A_0} \times 100$$

where A_0 is the absorbance of the pure DPPH solution at 517 nm and A_t the absorbance of the DPPH solution the after 3 h incubation with the films.

RESULTS AND DISCUSSION

Nanoparticle Synthesis. The lignin nanoparticles used in this study were prepared via precipitation as illustrated in

https://doi.org/10.1021/acsapm.2c00420
ACS Appl. Polym. Mater. 2022, 4, 4808−4817

Scheme 1.[40] To this end, lignin was dissolved in ethylene glycol, followed by addition of HCl and subsequent dialysis against water. The formation of nanoparticles via this process is driven by the change in pH as well as the addition of an antisolvent. The size and size distribution of the lignin nanoparticles were determined by atomic force microscopy (AFM). Figure 1A presents an AFM image of lignin nanoparticles deposited on a silicon substrate. Analysis of this AFM image reveals an average particle diameter of 110.8 ± 11.9 nm.

PLA-grafted lignin nanoparticles were prepared by organo-catalyzed ring-opening polymerization of DL-lactide using DBU as catalyst. Polymerizations were conducted in DCM at room temperature for a period of 3 h and at lactide/lignin nanoparticle ratios of 1, 5, 10, and 15 (w/w). AFM analysis of lignin nanoparticles that were dispersed in DCM for 3 h did not reveal significant changes in particle size, indicating that the nanoparticles are stable in the solvent that was used for the polymerization (Figure S2). The resulting PLA-grafted lignin nanoparticles were characterized with ^{1}H, DOSY, and ^{31}P NMR spectroscopy as well as AFM and UV−vis spectroscopy. Table 1 summarizes the results of these analyses.

Table 1. Degree of Polymerization and Number-Average Molecular Weight of the PLA Grafts and Lignin Content of PLA-Grafted Lignin Nanoparticles Prepared at Different Initial Lactide/Lignin Nanoparticle (LNP) Ratios

lactide:LNP (w/w)	PLA DP[a]	PLA M_n (Da)[a]	lignin (wt %)[b]	yield (%)
1	8	1108	30.4	65
5	27	3862	15.0	84
10	38	5472	8.8	87
15	73	10463	5.1	91

[a]Determined by ^{1}H NMR spectroscopy (spectra are presented in Figure S3). [b]Obtained from UV−vis spectroscopy.

Figure 2 compares ^{1}H NMR spectra recorded from lignin nanoparticles as well as PLA-grafted lignin nanoparticles that had been dissolved in DMF-d_7. ^{1}H NMR spectra of all synthesized PLA-grafted lignin nanoparticles are presented in Figure S3. The ^{1}H NMR spectrum obtained from the lignin nanoparticles shows resonances that can be assigned to aliphatic protons (0.5−1.7 ppm), aliphatic hydroxyl groups (3.2−3.6 ppm), methoxy groups (3.5−4.1 ppm), and aromatic H/phenolic hydroxyl groups (6.5−7.5 ppm).[42,43] The ^{1}H NMR spectrum of the PLA-grafted lignin nanoparticles presents additional resonances at 4.9 and 4.0 ppm, which are due to the C−H protons of the lactic acid repeat units, respectively, chain end of the PLA grafts, and a signal at 1.5 ppm that can be assigned to the PLA side-chain methyl groups. The number-average degree of polymerization and the number-average molecular weight of the PLA grafts were calculated by comparing the integrals of the CH resonances at 4.9 ppm with that of the CH proton at the terminal lactic acid unit at 4.0 ppm. As indicated in Table 1, the degree of polymerization of the PLA grafts increases gradually from 8 to 73 upon increasing the initial lactide/nanoparticle ratio that was used in the ring-opening polymerization from 1 to 15. With increasing degree of polymerization of the PLA grafts, the lignin content of the nanoparticles, as determined by UV−vis spectroscopy, decreases from 30 to 5 wt %.

The size and shape of the PLA-grafted lignin nanoparticles were studied by AFM. As an example, Figure 1B shows an AFM image obtained from PLA-grafted lignin nanoparticles that were prepared at an initial lactide/lignin nanoparticle ratio of 5/1. The AFM image shows that the particle shape is retained during the lactide ring-opening polymerization and reveals an increase in particle size from 110.8 ± 11.9 to 197.5 ± 31.8 nm. Results of AFM analyses of PLA-grafted nanoparticles obtained at all four lactide/lignin nanoparticle ratios are presented in Figure S4.

The PLA-grafted lignin nanoparticles were further characterized by DOSY and ^{31}P NMR spectroscopy. Figure S5 shows the DOSY-NMR spectrum of PLA-grafted lignin nanoparticles prepared with an initial lactide/lignin nanoparticle ratio of 15/1. The DOSY spectrum reveals similar diffusion coefficients for the characteristic lignin and PLA ^{1}H NMR resonances, which confirms the covalent attachment of the PLA grafts to the lignin nanoparticles. The spectrum also presents a lignin signal characterized by a larger diffusion coefficient, which is due to unmodified lignin that constitutes the interior of the nanoparticle and that is not modified with PLA.

The identity and number of lignin hydroxyl groups that serve as initiators for the lactide ring-opening polymerization can be quantitatively assessed by ^{31}P NMR spectroscopy. These analyses were performed on solutions of the PLA-grafted or unmodified lignin nanoparticles and use TMDP to phosphorylate unreacted hydroxyl groups. As an example, Figure S6 shows ^{31}P NMR spectra recorded from solutions of unmodified lignin nanoparticles as well as of PLA-grafted lignin nanoparticles that were prepared at an initial lactide/nanoparticle ratio of 15 to 1. The ^{31}P NMR spectrum of the unmodified lignin nanoparticles shows the signals of the aliphatic hydroxyl groups (145.5−148.5 ppm), phenolic hydroxyls (137.5−143.5 ppm), and carboxylic acids (133.5−135.2 ppm). Compared to the ^{31}P NMR spectrum of the unmodified nanoparticles, the spectrum of the PLA-grafted nanoparticles reveals a significant reduction in the resonances of both the aliphatic and phenolic hydroxyl groups. Quantitative analysis of the hydroxyl group concentration from these spectra indicates phenolic and aliphatic hydroxyl group concentrations of 3.24 and 1.82 mmol/g for the unmodified lignin nanoparticles, and 2.13 and 0.09 mmol/g for the PLA-grafted lignin nanoparticles. These results indicate that, as expected, the majority of the PLA grafts are grown from aliphatic hydroxyl groups as initiator.[43−45]

PLA Blend Film Preparation and Characterization. Blends of PLA and PLA-grafted lignin nanoparticles were obtained via solvent casting from chloroform. The PLA used for the preparation of these blends was a commercially available food packaging grade material. For the preparation of these blend films, PLA-grafted lignin nanoparticles were used that were obtained via ring-opening polymerization of lactide at an initial monomer/nanoparticle ratio of 5/1 (w/w). These particles were selected because they have a relatively high lignin content (15 wt %) and PLA grafts with a reasonable degree of polymerization, which was believed to facilitate compatibilization with the PLA blend matrix. The amount of PLA-grafted lignin nanoparticles was varied to generate a series of blend films containing 1, 5, and 10 wt % lignin. As control samples, blends of PLA with 1, 5, and 10 wt % lignin as well as blends of PLA and 1, 5, and 10 wt % unmodified lignin nanoparticles were prepared. Figure S7 shows optical micrographs of the different blend films.

https://doi.org/10.1021/acsapm.2c00420
ACS Appl. Polym. Mater. 2022, 4, 4808−4817

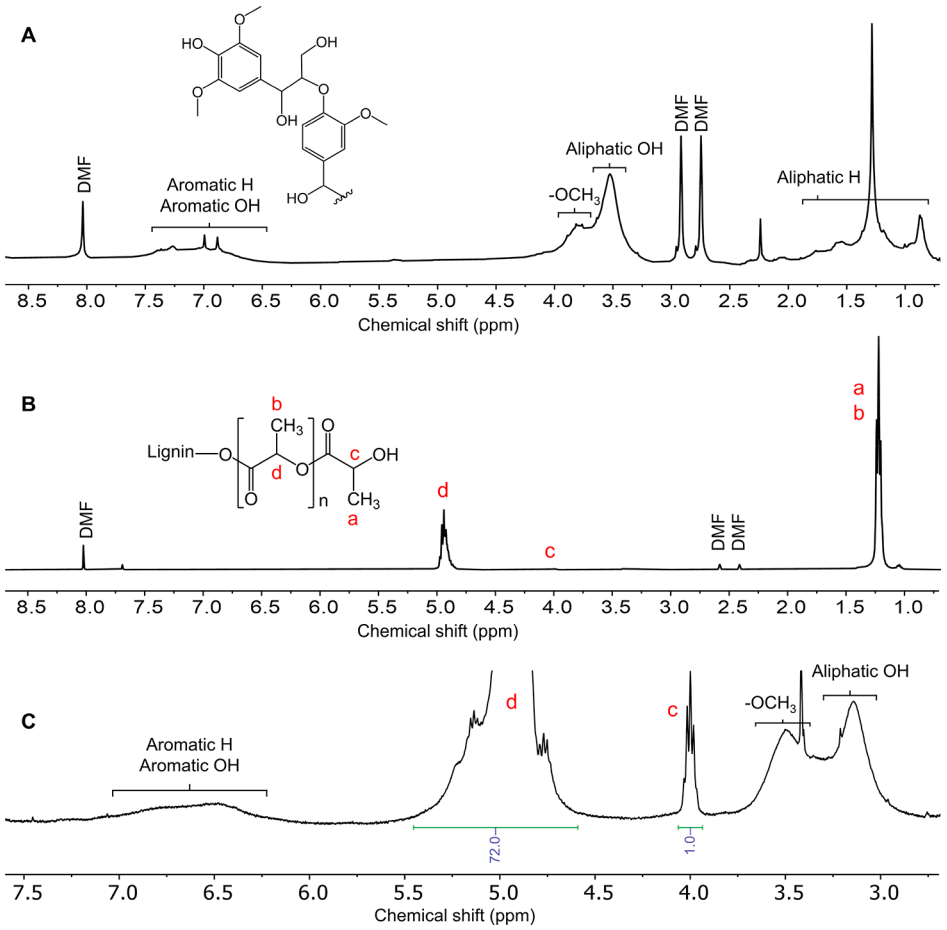

Figure 2. ^{1}H NMR spectra of lignin nanoparticles (A) and PLA-grafted lignin nanoparticles that were obtained at an initial lactide/lignin nanoparticle ratio of 15/1 (w/w) (B, C). Part C presents a magnification of the 2.5−7.5 ppm region of the spectrum shown in part B.

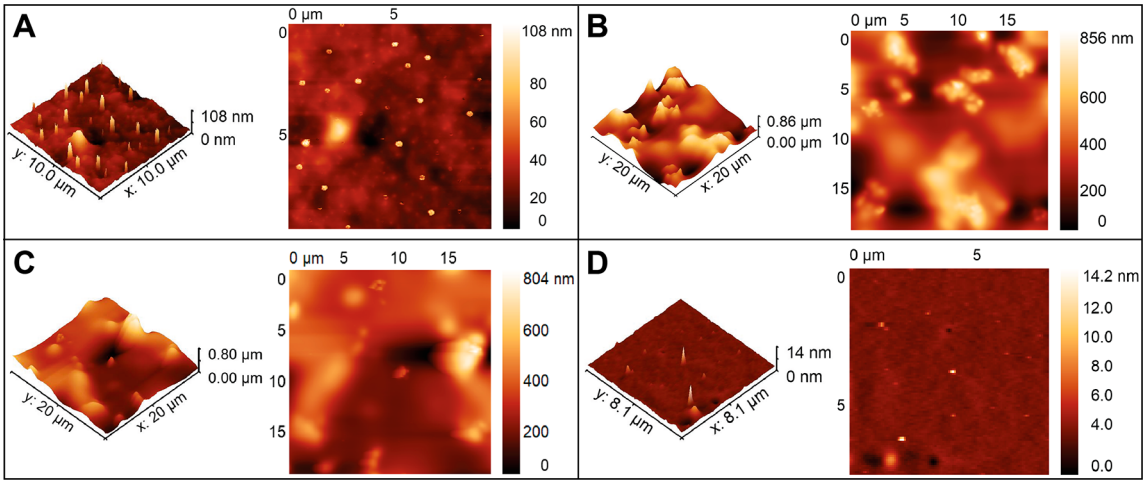

Figure 3. AFM images of spin-coated films of (A) a PLA−PLA-grafted lignin nanoparticle blend, (B) a PLA−lignin nanoparticle blend, (C) a PLA−lignin blend, and (D) neat PLA (all the blends contain 10 wt % lignin).

To investigate the dispersion of the lignin nanoparticles in the PLA blends, the films were studied by AFM. Figure 3 shows AFM images of spin-coated blend films of PLA and PLA-grafted lignin nanoparticles (Figure 3A), PLA and unmodified lignin nanoparticles (Figure 3B), PLA and lignin (Figure 3C) (all containing 10 wt % lignin), and a pure PLA film (Figure 3D). The AFM image of the PLA/PLA-grafted lignin nanoparticle blend film reveals ∼108 nm diameter nanoparticles that are well dispersed in the PLA matrix. The blend film prepared from PLA and unmodified lignin nanoparticles also shows the presence of nanoparticles. In contrast to the PLA-grafted lignin nanoparticles, however, the unmodified nanoparticles aggregate in micrometer-sized domains in the PLA matrix. Figure 3C illustrates the phase-separated structure of the PLA/lignin blend and Figure 3D the uniform film that is obtained by solution casting of pure PLA.

https://doi.org/10.1021/acsapm.2c00420
ACS Appl. Polym. Mater. 2022, 4, 4808−4817

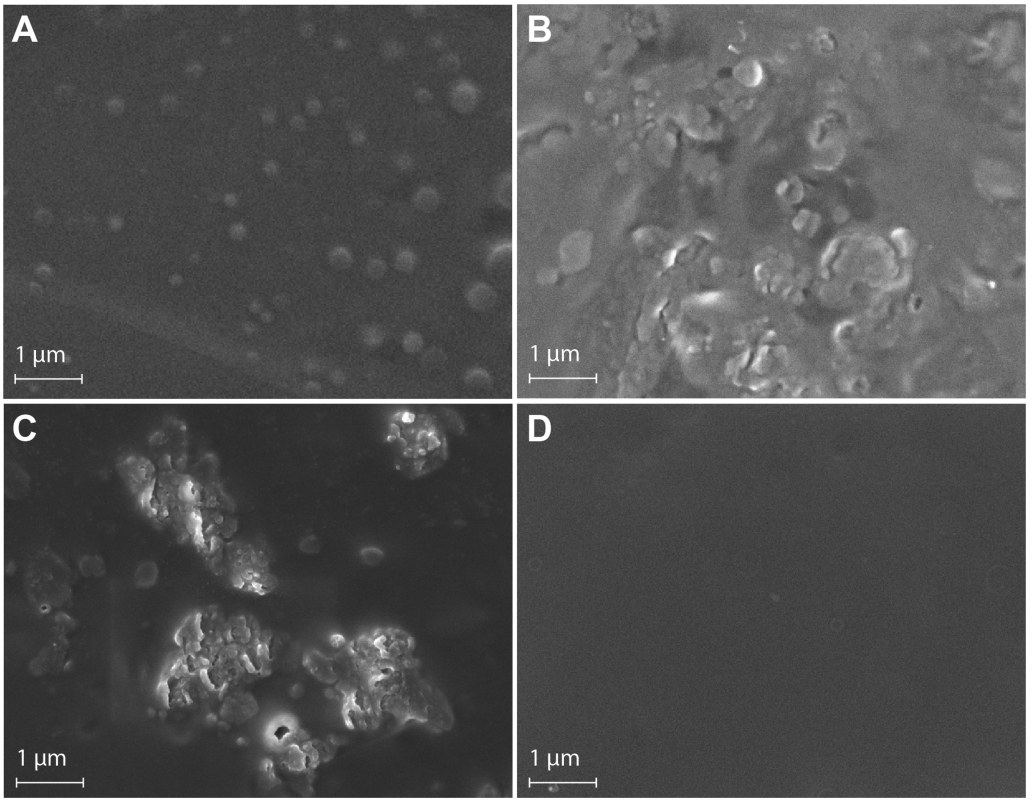

Figure 4. SEM images of 1 μm thick films prepared via ultramicrotomy of (A) a PLA−PLA-grafted lignin nanoparticle blend, (B) a PLA−lignin nanoparticle blend, (C) a PLA−lignin blend, and (D) neat PLA (all blends contain 10 wt % lignin).

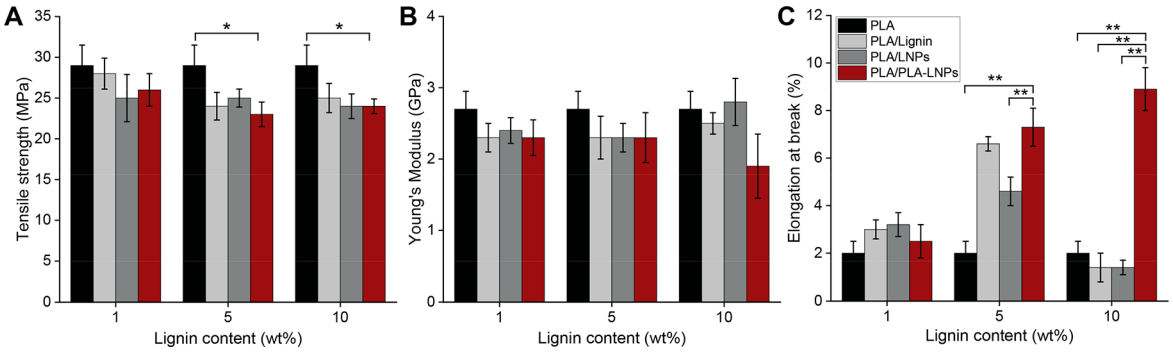

Figure 5. Tensile properties of pure PLA films and PLA blends containing lignin, lignin nanoparticles (LNPs), and PLA-grafted lignin nanoparticles (PLA-LNPs) with 1, 5, and 10 wt % lignin content: (A) tensile strength, (B) Young's modulus, and (C) elongation at break. Results and error bars correspond to the average and standard deviation of measurements performed on five different specimens (n = 5) for each sample. Statistical analysis was performed with the Student's t test (*p < 0.05, ** p < 0.01, ***p < 0.001).

The results of the AFM experiments were corroborated by SEM analysis of 1 μm thick microtomed specimens of the films (Figure 4). While the SEM image of the PLA/PLA-grafted lignin nanoparticle blend reveals well-dispersed nanoparticles, aggregation is observed in blends of PLA and the unmodified lignin nanoparticles. The SEM image in Figure 4C also shows that phase separation occurs in the PLA/lignin blend. Taken together, the results of the AFM and SEM analyses demonstrate that surface modification of lignin nanoparticles with PLA grafts provides an efficient strategy to ensure a uniform dispersion of lignin nanoparticles in the PLA matrix.

By use of DSC and TGA, the thermal properties of the PLA/PLA-grafted lignin nanoparticle, PLA/lignin nanoparticle, and PLA/lignin blends (all containing 10 wt % lignin) were analyzed and compared with those of pure PLA. The results of these analyses, which are presented in Figure S8 and Table S1, indicate that neither the glass transition temperature (T_g) nor the onset of thermal degradation of the PLA matrix was affected by the incorporation of 10 wt % lignin.

The mechanical properties of the PLA/PLA-grafted lignin nanoparticle, PLA/lignin nanoparticle, and PLA/lignin blends were investigated by tensile testing experiments and compared with those of pure PLA samples. Representative stress−strain curves of the different samples are presented in Figure S9. Figure 5 summarizes the tensile strength, Young's modulus, and elongation at break values obtained from these experiments. Pure PLA shows brittle behavior, with low elongation at break (about 2%) and a Young's modulus of ∼2.6 GPa. These values are in agreement with previously published data on PLA films prepared via solvent casting.[46] The tensile strength and

https://doi.org/10.1021/acsapm.2c00420
ACS Appl. Polym. Mater. 2022, 4, 4808−4817

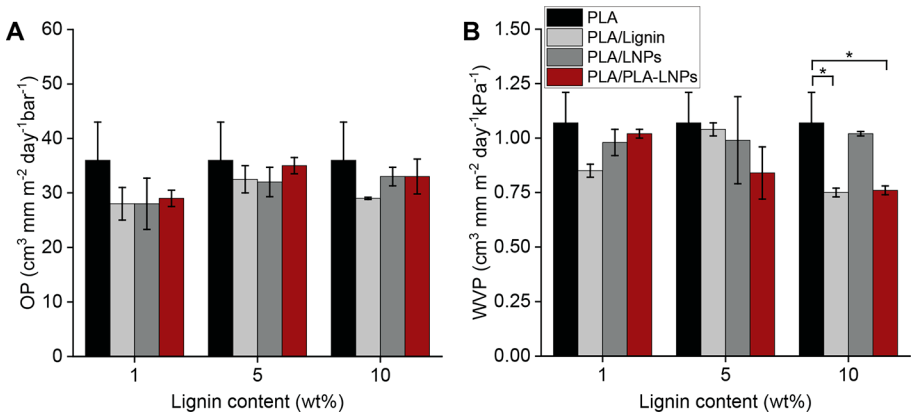

Figure 6. Gas barrier properties of pure PLA films and PLA blends containing lignin, lignin nanoparticles (LNPs), and PLA-grafted lignin nanoparticles (PLA-LNPs) with 1, 5, and 10 wt % lignin content: (A) oxygen permeability (OP) and (B) water vapor permeability (WVP). Results and error bars correspond to the average and standard deviation of measurements performed on two different samples (n = 2). Statistical analysis was performed with the Student's t test (*p < 0.05, **p < 0.01, ***p < 0.001).

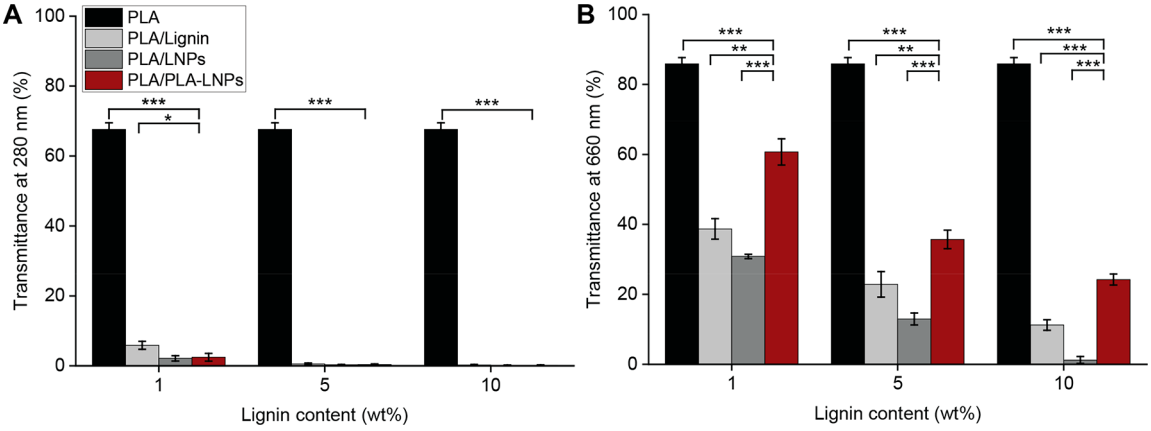

Figure 7. Transmittance (%) of pure PLA films and PLA blends containing lignin, lignin nanoparticles (LNPs), and PLA-grafted lignin nanoparticles (PLA-LNPs) with 1, 5, and 10 wt % lignin content, recorded at (A) 280 nm and (B) 660 nm. Results and error bars correspond to the average and standard deviation of measurements performed on three different specimens (n = 3) for each sample. Statistical analysis was performed with Student's t test (*p < 0.05, **p < 0.01, ***p < 0.001).

Young's modulus of the blends slightly decreased compared to neat PLA, but neither significantly varied across the different lignin contents or across the type of filler (lignin, unmodified lignin nanoparticles, PLA-grafted lignin nanoparticles). The elongation at break of the blend samples increased when 1 wt % filler was incorporated and even further upon increasing the lignin content to 5 wt % for all three types of PLA/lignin blends. Further increasing the lignin content to 10 wt %, however, resulted in a decrease in elongation at break for the PLA/lignin and PLA/lignin nanoparticle blends, probably due to phase separation and the low cohesion between lignin and PLA in these samples. Blends of PLA and PLA-grafted nanoparticles, in contrast, showed a further increase in elongation at break upon increasing the lignin content from 5 to 10 wt %. This is attributed to the presence of the grafted PLA chains that act as compatibilizers.

As a food packaging material, PLA serves to prevent exposure of food to oxygen and water vapor. PLA presents moderate oxygen barrier properties and relatively poor water vapor barrier properties.[47,48] To evaluate the gas barrier properties of the blend films and assess the impact of the incorporation of the different lignin fillers, the oxygen and water vapor transmission rates (Figure S10) as well as permeability (Figure 6) of the different PLA/lignin blends films were measured and compared with that of pure PLA. The results presented in Figure 6 demonstrate that the oxygen permeability of the PLA films was not significantly influenced by the incorporation of the lignin-based fillers. In contrast, comparison of the water vapor permeabilities reveals a slight reduction in water vapor permeability of the blends as compared to pure PLA in most cases, with a significant reduction for films that contain lignin or PLA-grafted nanoparticles at a lignin content of 10 wt %.

In addition to providing a barrier to oxygen and water vapor exposure, food packaging films also need to possess appropriate optical properties. On the one hand, customers desire to see the product inside the package. On the other hand, exposure to UV light can induce degradation of lipids, proteins, and vitamins, thus reducing the food shelf life.[49] An optimal packaging material should hence provide UV-protection to the food, while maintaining the product visible by the naked eye. The optical properties of PLA blend films with thicknesses of 0.8−1 mm were investigated using UV−vis spectroscopy by measuring the percent transmittance of light at 280 nm (T_{280}) and 660 nm (T_{660}), respectively (Figure 7). Figure S7 presents optical micrographs of the different blend films. Figure S11A shows the UV−vis transmittance spectra of the films recorded between 200 and 800 nm. These spectra

https://doi.org/10.1021/acsapm.2c00420
ACS Appl. Polym. Mater. 2022, 4, 4808−4817

show that neat PLA is highly transparent in both the visible and UV spectral regions, with high transmittance at wavelengths above 240 nm. As indicated in Figure 7A, blending PLA with 1 wt % lignin, in contrast, reduces the UV light transmittance at 280 nm to <10%, and further increasing the lignin content of the blends to 10 wt % almost completely blocks UV-light transmittance ($T_{280} \sim 0.2\%$) (see also Figure S12). At the same time, however, the different PLA/lignin blends (especially at low lignin content) retained a relatively high transmittance in the visible light region (Figure 7B). At all the investigated lignin contents, blends of PLA and PLA-grafted lignin nanoparticles showed a higher transparency in the visible range as compared to PLA/lignin nanoparticle blend films or PLA/lignin blend films, which reflects the uniform distribution of the PLA-grafted lignin nanoparticles in the PLA matrix and the phase separation and aggregation that occurs in the PLA/lignin nanoparticles and PLA/lignin blends. The results presented in Figure 7 reflect the optical micrographs of the blends that are presented in Figure S7 and which also demonstrate that even at relatively high lignin contents PLA blends with PLA-grafted lignin nanoparticles appear more transparent as compared to blends of PLA with lignin nanoparticles or lignin.

In a final set of experiments, the antioxidant activity of the blend films was evaluated. Oxygen radical species generated by thermal processing or irradiation of packaging and food can initiate the oxidation of lipids, vitamins, and proteins in the packaged product, thus drastically reducing its shelf life.[14,50,51] The antioxidant activity of the films was measured with the DPPH assay.[41] DPPH is a stable free radical that shows a strong absorbance at 517 nm. DPPH can act as a radical scavenger and upon reaction with another radical becomes colorless. Figure S11B presents UV−vis spectra of DPPH solutions upon exposure to films of PLA and the different PLA/lignin blends. From the decrease of the intensity of the absorbance at 517 nm, a DPPH conversion can be calculated, which is taken as a measure of the antioxidant activity of the films. Figure 8 compares the antioxidant activities of pure PLA

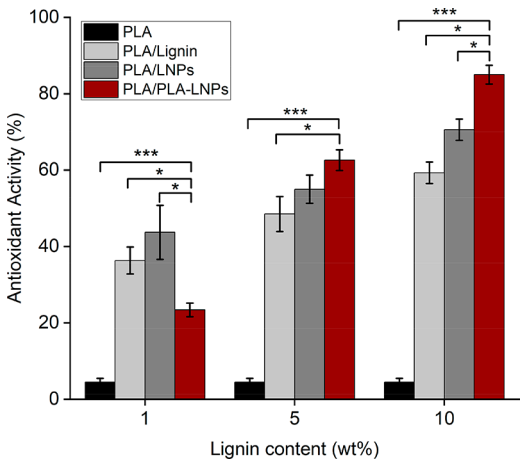

Figure 8. Antioxidant activity of pure PLA films and PLA blends containing lignin, lignin nanoparticles (LNPs), and PLA-grafted lignin nanoparticles (PLA-LNPs) with 0, 1, 5, and 10 wt % lignin content, obtained by the DPPH assay. Results and error bars correspond to the average and standard deviation of measurements performed on three different specimens ($n = 3$). Statistical analysis was performed with the Student's t test (*$p < 0.05$, **$p < 0.01$, ***$p < 0.001$).

with that of the different PLA/lignin blend samples. While the pure PLA film only displays a low radical scavenging activity, blending as little as 1 wt % lignin strongly increases the antioxidant activity of the film. For each of the different PLA/lignin blend films, the antioxidant activity increases with increasing the lignin content. At low lignin contents (1 wt %), the PLA/lignin nanoparticle and PLA/lignin blend films outperform the PLA/PLA-grafted lignin nanoparticle blends. This is attributed to the fact that at these low lignin contents the lignin nanoparticles and the lignin are reasonably well dispersed in the PLA matrix, and the larger number of free hydroxyl groups present in the unmodified lignin nanoparticles and the free lignin dominate the better dispersion of the PLA-modified lignin nanoparticles, which carry a smaller number of free hydroxyl groups since part of these have been consumed as initiating sites for the lactide ring-opening polymerization. For blends that contain 5 and 10 wt % lignin, in contrast, the antioxidant activity of the PLA-grafted nanoparticle-containing films is higher as compared to that of the PLA/lignin nanoparticles and PLA/lignin blends. At these lignin contents in the blend, the effects of the phase separation of lignin and the aggregation of lignin nanoparticles become noticeable, whereas the PLA-grafted lignin nanoparticles remain well dispersed, resulting in a higher antioxidant activity in spite of the reduced number of free hydroxyl groups present in the PLA-grafted lignin nanoparticles.

CONCLUSIONS

This work has investigated the use of PLA-grafted lignin nanoparticles to enhance the antioxidant activity as well as the mechanical and barrier properties of PLA food packaging films. Lignin nanoparticles with sizes of ∼110 nm, which were obtained via precipitation, could be modified in a straightforward fashion with PLA grafts of various molecular weights via organocatalyzed ring-opening polymerization of lactide. Atomic force microscopy and scanning electron microscopy analyses revealed that these PLA-grafted nanoparticles could be uniformly dispersed in PLA to generate PLA−lignin blends with lignin contents of up to 10 wt % without any indication of nanoparticle aggregation. Analyses of blends of PLA with lignin or unmodified lignin nanoparticles, in contrast, revealed phase separation and nanoparticle aggregation. The incorporation of PLA-grafted nanoparticles allowed to efficiently reduce the optical transmittance of PLA in the UV range, while retaining reasonable transparency to the visible light region. Compared to blending lignin or unmodified lignin nanoparticles, incorporation of the PLA-grafted nanoparticles improved visible light transmission, highlighting the importance of avoiding phase separation and nanoparticle aggregation and reflecting the uniform dispersion of the PLA-grafted lignin nanoparticles. Blending PLA-grafted lignin nanoparticles also greatly improves the antioxidant properties of PLA. In particular at high lignin blend contents (5 and 10 wt %), the antioxidant activity of PLA−PLA-grafted nanoparticle blend films was found to be superior to that of PLA−lignin and PLA−lignin nanoparticle blends, which is also attributed to phase separation and nanoparticle aggregation in the latter two blend films.

ASSOCIATED CONTENT

Supporting Information

The Supporting Information is available free of charge at https://pubs.acs.org/doi/10.1021/acsapm.2c00420.

https://doi.org/10.1021/acsapm.2c00420
ACS Appl. Polym. Mater. 2022, 4, 4808−4817

Initial thermal degradation temperature and glass transition temperature; UV−vis absorbance spectra of DMF solutions of lignin nanoparticles and corresponding calibration curve; AFM images of the nanoparticles; ^{1}H NMR spectra of PLA-grafted lignin nanoparticles prepared with different lactide/lignin nanoparticle ratios; DOSY-NMR spectrum of PLA-grafted lignin nanoparticles; ^{31}P NMR spectra of nanoparticles before and after PLA grafting; photographs of the films; DSC and TGA curves; stress−strain curves obtained during tensile tests; oxygen and water vapor transmission rates; UV−vis transmission spectra of the films; magnification of Figure 7A (PDF)

AUTHOR INFORMATION

Corresponding Author

Harm-Anton Klok − *Institut des Matériaux and Institut des Sciences et Ingénierie Chimiques, Laboratoire des Polymères, École Polytechnique Fédérale de Lausanne (EPFL), CH-1015 Lausanne, Switzerland;* orcid.org/0000-0003-3365-6543; Phone: + 41 21 693 4866; Email: harm-anton.klok@epfl.ch

Authors

Alice Boarino − *Institut des Matériaux and Institut des Sciences et Ingénierie Chimiques, Laboratoire des Polymères, École Polytechnique Fédérale de Lausanne (EPFL), CH-1015 Lausanne, Switzerland*

Aigoul Schreier − *Institut des Matériaux, Laboratory for Processing of Advanced Composites, École Polytechnique Fédérale de Lausanne (EPFL), CH-1015 Lausanne, Switzerland*

Yves Leterrier − *Institut des Matériaux, Laboratory for Processing of Advanced Composites, École Polytechnique Fédérale de Lausanne (EPFL), CH-1015 Lausanne, Switzerland;* orcid.org/0000-0002-0532-0543

Complete contact information is available at: https://pubs.acs.org/10.1021/acsapm.2c00420

Notes

The authors declare no competing financial interest.

ACKNOWLEDGMENTS

This work was financially supported by the Swiss National Science Foundation (SNSF). The authors thank Lucie Navratilova from the Interdisciplinary Center for Electron Microscopy at EPFL for her help with the SEM analyses.

REFERENCES

(1) Geyer, R.; Jambeck, J. R.; Law, K. L. Production, Use, and Fate of All Plastics Ever Made. *Science Advances* **2017**, *3* (7), e1700782.

(2) Ritchie, H.; Roser, M. Plastic Pollution, www.ourworldindata.org/plastic-pollution.

(3) Sangroniz, A.; Zhu, J.-B.; Tang, X.; Etxeberria, A.; Chen, E. Y.-X.; Sardon, H. Packaging Materials with Desired Mechanical and Barrier Properties and Full Chemical Recyclability. *Nat. Commun.* **2019**, *10* (1), 3559.

(4) Bioplastics Market Development Update 2020. www.european-bioplastics.org, 2020 (accessed 2021-12-10).

(5) Drumright, R. E.; Gruber, P. R.; Henton, D. E. Polylactic Acid Technology. *Adv. Mater.* **2000**, *12* (23), 1841−1846.

(6) Arrieta, M.; Samper, M.; Aldas, M.; López, J. On the Use of PLA-PHB Blends for Sustainable Food Packaging Applications. *Materials* **2017**, *10* (9), 1008.

(7) https://www.fda.gov/ (accessed 2022-01-18).

(8) Iheaturu, N. C.; Nwakaudu, A. A.; Nwakaudu, M. S.; Owuamanam, C. I. The Use of Natural Antioxidant Active Polymer Packaging for Food Preservation: A Review. *Futo Journal Series* **2018**, *4*, 94−112.

(9) Dassarma, B.; Nandi, D. K.; Gangopadhyay, S.; Samanta, S. Hepatoprotective Effect of Food Preservatives (Butylated Hydroxyanisole, Butylated Hydroxytoluene) on Carbon Tetrachloride-Induced Hepatotoxicity in Rat. *Toxicology Reports* **2018**, *5*, 31−37.

(10) Vally, H.; Misso, N. L. Adverse Reactions to the Sulphite Additives. *Gastroenterol Hepatol Bed Bench* **2012**, *5* (1), 16−23.

(11) Cantwell, M.; Elliott, C. Nitrates, Nitrites and Nitrosamines from Processed Meat Intake and ColorectalCancer Risk. *J. Clin. Nutr. Diet.* **2017**, DOI: 10.4172/2472-1921.100062.

(12) Lu, F.; Chu, L.; Gau, R. Free Radical-scavenging Properties of Lignin. *Nutrition and Cancer* **1998**, *30* (1), 31−38.

(13) Dizhbite, T. Characterization of the Radical Scavenging Activity of Lignins-Natural Antioxidants. *Bioresour. Technol.* **2004**, *95* (3), 309−317.

(14) Domenek, S.; Louaifi, A.; Guinault, A.; Baumberger, S. Potential of Lignins as Antioxidant Additive in Active Biodegradable Packaging Materials. *J. Polym. Environ* **2013**, *21* (3), 692−701.

(15) Stewart, D. Lignin as a Base Material for Materials Applications: Chemistry, Application and Economics. *Industrial Crops and Products* **2008**, *27* (2), 202−207.

(16) Upton, B. M.; Kasko, A. M. Strategies for the Conversion of Lignin to High-Value Polymeric Materials: Review and Perspective. *Chem. Rev.* **2016**, *116* (4), 2275−2306.

(17) Witzler, M.; Alzagameem, A.; Bergs, M.; Khaldi-Hansen, B. E.; Klein, S. E.; Hielscher, D.; Kamm, B.; Kreyenschmidt, J.; Tobiasch, E.; Schulze, M. Lignin-Derived Biomaterials for Drug Release and Tissue Engineering. *Molecules* **2018**, *23* (8), 1885.

(18) Sugiarto, S.; Leow, Y.; Tan, C. L.; Wang, G.; Kai, D. How Far Is Lignin from Being a Biomedical Material? *Bioactive Materials* **2022**, *8*, 71−94.

(19) Miao, Y.; Tang, Z.; Zhang, Q.; Reheman, A.; Xiao, H.; Zhang, M.; Liu, K.; Huang, L.; Chen, L.; Wu, H. Biocompatible Lignin-Containing Hydrogels with Self-Adhesion, Conductivity, UV Shielding, and Antioxidant Activity as Wearable Sensors. *ACS Appl. Polym. Mater.* **2022**, *4* (2), 1448−1456.

(20) Sadeghifar, H.; Ragauskas, A. Lignin as a UV Light Blocker—A Review. *Polymers* **2020**, *12* (5), 1134.

(21) Shu, F.; Jiang, B.; Yuan, Y.; Li, M.; Wu, W.; Jin, Y.; Xiao, H. Biological Activities and Emerging Roles of Lignin and Lignin-Based Products - A Review. *Biomacromolecules* **2021**, *22* (12), 4905−4918.

(22) Yao, J.; Odelius, K.; Hakkarainen, M. Microwave Hydrophobized Lignin with Antioxidant Activity for Fused Filament Fabrication. *ACS Appl. Polym. Mater.* **2021**, *3* (7), 3538−3548.

(23) Kai, D.; Ren, W.; Tian, L.; Chee, P. L.; Liu, Y.; Ramakrishna, S.; Loh, X. J. Engineering Poly(Lactide)−Lignin Nanofibers with Antioxidant Activity for Biomedical Application. *ACS Sustainable Chem. Eng.* **2016**, *4* (10), 5268−5276.

(24) Domínguez-Robles, J.; Martin, N.; Fong, M.; Stewart, S.; Irwin, N.; Rial-Hermida, M.; Donnelly, R.; Larrañeta, E. Antioxidant PLA Composites Containing Lignin for 3D Printing Applications: A Potential Material for Healthcare Applications. *Pharmaceutics* **2019**, *11* (4), 165.

(25) Park, C.-W.; Youe, W.-J.; Kim, S.-J.; Han, S.-Y.; Park, J.-S.; Lee, E.-A.; Kwon, G.-J.; Kim, Y.-S.; Kim, N.-H.; Lee, S.-H. Effect of Lignin Plasticization on Physico-Mechanical Properties of Lignin/Poly-(Lactic Acid) Composites. *Polymers* **2019**, *11* (12), 2089.

(26) Shankar, S.; Rhim, J.-W.; Won, K. Preparation of Poly-(Lactide)/Lignin/Silver Nanoparticles Composite Films with UV Light Barrier and Antibacterial Properties. *Int. J. Biol. Macromol.* **2018**, *107*, 1724−1731.

(27) Chung, Y.-L.; Olsson, J. V.; Li, R. J.; Frank, C. W.; Waymouth, R. M.; Billington, S. L.; Sattely, E. S. A Renewable Lignin−Lactide Copolymer and Application in Biobased Composites. *ACS Sustainable Chem. Eng.* **2013**, *1* (10), 1231−1238.
(28) Guo, J.; Chen, X.; Wang, J.; He, Y.; Xie, H.; Zheng, Q. The Influence of Compatibility on the Structure and Properties of PLA/Lignin Biocomposites by Chemical Modification. *Polymers* **2020**, *12* (1), 56.
(29) Kumar, A.; Tumu, V. R.; Ray Chowdhury, S.; S.V.S., R. R. A Green Physical Approach to Compatibilize a Bio-Based Poly (Lactic Acid)/Lignin Blend for Better Mechanical, Thermal and Degradation Properties. *Int. J. Biol. Macromol.* **2019**, *121*, 588−600.
(30) Sun, Y.; Ma, Z.; Xu, X.; Liu, X.; Liu, L.; Huang, G.; Liu, L.; Wang, H.; Song, P. Grafting Lignin with Bioderived Polyacrylates for Low-Cost, Ductile, and Fully Biobased Poly(Lactic Acid) Composites. *ACS Sustainable Chem. Eng.* **2020**, *8* (5), 2267−2276.
(31) Spiridon, I.; Tanase, C. E. Design, Characterization and Preliminary Biological Evaluation of New Lignin-PLA Biocomposites. *Int. J. Biol. Macromol.* **2018**, *114*, 855−863.
(32) Yang, W.; Fortunati, E.; Dominici, F.; Giovanale, G.; Mazzaglia, A.; Balestra, G. M.; Kenny, J. M.; Puglia, D. Effect of Cellulose and Lignin on Disintegration, Antimicrobial and Antioxidant Properties of PLA Active Films. *Int. J. Biol. Macromol.* **2016**, *89*, 360−368.
(33) Yang, W.; Fortunati, E.; Dominici, F.; Giovanale, G.; Mazzaglia, A.; Balestra, G. M.; Kenny, J. M.; Puglia, D. Synergic Effect of Cellulose and Lignin Nanostructures in PLA Based Systems for Food Antibacterial Packaging. *Eur. Polym. J.* **2016**, *79*, 1−12.
(34) Yang, W.; Fortunati, E.; Dominici, F.; Kenny, J. M.; Puglia, D. Effect of Processing Conditions and Lignin Content on Thermal, Mechanical and Degradative Behavior of Lignin Nanoparticles/Polylactic (Acid) Bionanocomposites Prepared by Melt Extrusion and Solvent Casting. *Eur. Polym. J.* **2015**, *71*, 126−139.
(35) Yang, W.; Dominici, F.; Fortunati, E.; Kenny, J. M.; Puglia, D. Effect of Lignin Nanoparticles and Masterbatch Procedures on the Final Properties of Glycidyl Methacrylate- g -Poly (Lactic Acid) Films before and after Accelerated UV Weathering. *Industrial Crops and Products* **2015**, *77*, 833−844.
(36) Cavallo, E.; He, X.; Luzi, F.; Dominici, F.; Cerrutti, P.; Bernal, C.; Foresti, M. L.; Torre, L.; Puglia, D. UV Protective, Antioxidant, Antibacterial and Compostable Polylactic Acid Composites Containing Pristine and Chemically Modified Lignin Nanoparticles. *Molecules* **2021**, *26* (1), 126.
(37) Iglesias Montes, M. L.; Luzi, F.; Dominici, F.; Torre, L.; Cyras, V. P.; Manfredi, L. B.; Puglia, D. Design and Characterization of PLA Bilayer Films Containing Lignin and Cellulose Nanostructures in Combination With Umbelliferone as Active Ingredient. *Front. Chem.* **2019**, *7*, 157.
(38) Karasu, F.; Müller, L.; Ridaoui, H.; Ibn ElHaj, M.; Flodberg, G.; Aulin, C.; Axrup, L.; Leterrier, Y. Organic-Inorganic Hybrid Planarization and Water Vapor Barrier Coatings on Cellulose Nanofibrils Substrates. *Front. Chem.* **2018**, *6*, 571.
(39) Aulin, C.; Ström, G. Multilayered Alkyd Resin/Nanocellulose Coatings for Use in Renewable Packaging Solutions with a High Level of Moisture Resistance. *Ind. Eng. Chem. Res.* **2013**, *52* (7), 2582−2589.
(40) Frangville, C.; Rutkevičius, M.; Richter, A. P.; Velev, O. D.; Stoyanov, S. D.; Paunov, V. N. Fabrication of Environmentally Biodegradable Lignin Nanoparticles. *ChemPhysChem* **2012**, *13*, 4235−4243.
(41) Blois, M. S. Antioxidant Determinations by the Use of a Stable Free Radical. *Nature* **1958**, *181* (4617), 1199−1200.
(42) Zhao, X.; Huang, Z.; Zhang, Y.; Yang, M.; Chen, D.; Huang, K.; Hu, H.; Huang, A.; Qin, X.; Feng, Z. Efficient Solid-Phase Synthesis of Acetylated Lignin and a Comparison of the Properties of Different Modified Lignins. *J. Appl. Polym. Sci.* **2017**.
(43) Ren, W.; Pan, X.; Wang, G.; Cheng, W.; Liu, Y. Dodecylated Lignin-g-PLA for Effective Toughening of PLA. *Green Chem.* **2016**, *18* (18), 5008−5014.
(44) Zhang, X.; MacDonald, D. A.; Goosen, M. F. A.; McAuley, K. B. Mechanism of Lactide Polymerization in the Presence of Stannous Octoate: The Effect of Hydroxy and Carboxylic Acid Substances. *J. Polym. Sci. A Polym. Chem.* **1994**, *32* (15), 2965−2970.
(45) Kamber, N. E.; Jeong, W.; Waymouth, R. M.; Pratt, R. C.; Lohmeijer, B. G. G.; Hedrick, J. L. Organocatalytic Ring-Opening Polymerization. *Chem. Rev.* **2007**, *107* (12), 5813−5840.
(46) Gordobil, O.; Egüés, I.; Labidi, J. Modification of Eucalyptus and Spruce Organosolv Lignins with Fatty Acids to Use as Filler in PLA. *React. Funct. Polym.* **2016**, *104*, 45−52.
(47) Lehermeier, H. J.; Dorgan, J. R.; Way, J. D. Gas Permeation Properties of Poly(Lactic Acid). *J. Membr. Sci.* **2001**, *190* (2), 243−251.
(48) Sonchaeng, U.; Iñiguez-Franco, F.; Auras, R.; Selke, S.; Rubino, M.; Lim, L.-T. Poly(Lactic Acid) Mass Transfer Properties. *Prog. Polym. Sci.* **2018**, *86*, 85−121.
(49) Duncan, S. E.; Hannah, S. Light-Protective Packaging Materials for Foods and Beverages. In *Emerging Food Packaging Technologies*; Elsevier: 2012; pp 303−322.
(50) Halliwell, B.; Murcia, M. A.; Chirico, S.; Aruoma, O. I. Free Radicals and Antioxidants in Food and in Vivo: What They Do and How They Work. *Critical Reviews in Food Science and Nutrition* **1995**, *35* (1−2), 7−20.
(51) Sun, Y.-E.; Wang, W.-D.; Chen, H.-W.; Li, C. Autoxidation of Unsaturated Lipids in Food Emulsion. *Critical Reviews in Food Science and Nutrition* **2011**, *51* (5), 453−466.

https://doi.org/10.1021/acsapm.2c00420
ACS Appl. Polym. Mater. 2022, 4, 4808−4817